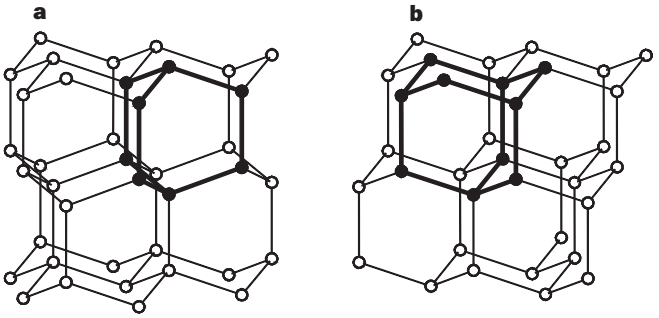

Figure 4 The structures of the ice phases I_h (**a**) and I_c (**b**). Oxygen atoms are shown as circles and hydrogen bonds are represented as lines. The darkened portions depict the smallest representative structural motif in each case. The hexagonal phase I_h is formed when water is cooled below its freezing point at atmospheric pressure. The cubic phase I_c can be formed by condensation of water vapour below –80 °C, or via a phase transition from vitreous ice or ices II, III or V. Above –80 °C, ice I_c itself transforms irreversibly to ice I_h. In both instances, each oxygen atom is situated at the centre of a tetrahedral arrangement of its four nearest-neighbour molecules. Its hydrogen atoms and lone pairs of electrons are directed towards these neighbours, thus facilitating the formation of four hydrogen bonds per water molecule, with each molecule acting as a double donor as well as a double acceptor. In each case, the lattice consists of two-dimensional layers of hexagonal rings in the chair conformation. These puckered sheets are stacked on one another, and are interconnected by the formation of hexagonal rings composed of three molecules each form adjacent layers. The two forms of ice I differ only in the stacking sequence of the puckered layers relative to one another, such that the interconnecting rings are in the boat conformation in ice I_h, while they assume the chair conformation in ice I_c.

techniques has afforded a relatively clear understanding of the structure of water in the solid state, and 12 polymorphic forms of ice, denoted as I_h, I_c and II–XI, have been characterized to date. Phases I_h and I_c are the two most common forms of ice and are strikingly similar in structure (Fig. 4). Extended water aggregates are also encountered in multi-component crystals and well-known examples include biological macromolecules[15] and clathrate hydrates[16]. We also note that a recent study has produced a solid-state structure which is stabilized by an infinite two-dimensional ice-like framework intercalated between $CdNi(CN)_4$ layers[17].

An improved understanding of the three-dimensional structural aspects of water has important implications in the area of structural biology. Indeed, investigations of the forces at play in macromolecular interactions[18] have demonstrated the importance of water structuring, and this point has been illustrated by several examples including the structures of *Scapharca* dimeric haemoglobin[19], crambin[20], actinidin[21] and carbonic anhydrase C (ref. 22). There is much evidence that alludes to the presence of ordered water clusters in the active clefts of these proteins, but unambiguous positional information is still rare. It is thought that water molecules contribute to the complex stability by mediating hydrogen bonds between the functional groups of the protein and the ligands, and by filling potential voids or holes inside the binding site[23].

The structure reported here demonstrates that the ice I_c arrangement can be a favourable conformation for a water cluster in a mixed-component system, even at room temperature. It also shows how the cluster and its surroundings assume a complementary relationship, resulting in the void available to the cluster being optimally occupied both in terms of packing efficiency and the maximization of intermolecular interactions. □

Received 5 February; accepted 6 April 1998.

1. Lehn, J.-M. *Supramolecular Chemistry: Concepts and Perspectives* (VCH, Weinheim, 1995).
2. Lehn, J.-M. Supramolecular chemistry. *Science* **260,** 1762–1763 (1993).
3. Seto, C. T. & Whitesides, G. M. Molecular self-assembly through hydrogen bonding: Supramolecular aggregates based on the cyanuric acid · melamine lattice. *J. Am. Chem. Soc.* **115,** 905–916 (1993).
4. Wyler, R., de Mendoza, J. & Rebek, J. A synthetic cavity assembles through self-complementary hydrogen bonds. *Angew. Chem. Int. Edn Engl.* **32,** 1699–1701 (1993).
5. Hasenknopf, B., Lehn, J.-M., Kneisel, B., Baum, O. G. & Fenske, D. Self-assembly of a circular double helicate. *Angew. Chem. Int. Edn Engl.* **35,** 1838–1840 (1996).
6. Oriol, J. *et al*. A designed non-peptidic receptor that mimics the phosphocholine binding site of the McPC603 antibody. *Angew. Chem. Int. Edn Engl.* **35,** 1712–1715 (1996).
7. Dehl, R. E. & Hoeve, C. A. Broad-line NMR study of H_2O and D_2O in collagen fibres. *J. Chem. Phys.* **50,** 3245–3251 (1969).
8. Migchelsen, C., Berendsen, H. J. C. & Rupprecht, A. Hydration of DNA. Comparison of nuclear magnetic resonance results for oriented DNA in the *A*, *B* and *C* form. *J. Mol. Biol.* **37,** 235–237 (1968).
9. Steckel, F. & Szapiro, S. Physical properties of heavy oxygen water. Part I–Density and thermal expansion. *Trans. Faraday Soc.* **59,** 331–343 (1963).
10. Colson, S. D. & Dunning, T. H. The structure of Nature's solvent: water. *Science* **265,** 43–44 (1994).
11. Liu, K., Cruzan, J. D. & Saykally, R. J. Water clusters. *Science* **271,** 929–933 (1996).
12. König, H. A cubic ice modification. *Z. Kristallogr.* **105,** 279–286 (1944).
13. Eisenberg, D. & Kauzmann, W. *The Structure and Properties of Water* (Oxford Univ. Press, New York, 1969).
14. Franks, F. (ed.) *Water: A Comprehensive Treatise* Vols 1–4 (Plenum, New York, 1972).
15. Westhoff, E. (ed.) *Water and Biological Macromolecules* (CRC Press, Boca Raton, 1993).
16. Jeffrey, G. A. in *Inclusion Compounds* Vol. 1 (eds Atwood, J. L., Davies, J. E. D. & MacNicol, D. D.) Ch. 5 (Academic, London, 1984).
17. Park, K.-M., Kurodo, R. & Iwamoto, T. A two-dimensional ice with the topography of edge-sharing hexagons intercalated between $CdNi(CN)_4$ layers. *Angew. Chem. Int. Edn Engl.* **32,** 884–886 (1993).
18. Rau, D. C. & Parsegian, V. A. Direct measurement of forces between linear polysaccharides Xanthan and Schizophyllan. *Science* **249,** 1278–1281 (1990).
19. Royer, W. E., Pardanani, A., Gibson, Q. H., Peterson, E. S. & Feldman, J. M. Ordered water molecules as key allosteric mediators in a cooperative dimeric hemoglobin. *Proc. Natl Acad. Sci. USA* **93,** 14526–14531 (1996).
20. Teeter, M. M. Water structure of a hydrophobic protein at atomic resolution: Pentagon rings of water molecules in crystals of crambin. *Proc. Natl Acad. Sci. USA* **81,** 6014–6018 (1984).
21. Baker, E. N. Structure of actinidin, after refinement at 1.7 Å resoution. *J. Mol. Biol.* **141,** 441–484 (1980).
22. Liljas, A. *et al.* Crystal structure of human carbonic anhydrase C. *Nature New Biol.* **235,** 131–137 (1972).
23. Quiocho, F. A., Wilson, D. K. & Vyas, N. K. Substrate specificity and affinity of a protein modulated by bound water molecules. *Nature* **340,** 404–407 (1989).

Supplementary information is available on *Nature*'s World-Wide Web site (http://www.nature.com) or as paper copy from the London editorial office of *Nature*.

Acknowledgements. We thank C. Barnes for assistance with the unit cell and space group determination. This work was supported by the US NSF.

Correspondence and requests for materials should be addressed to J.L.A. (e-mail: chemja@mizzou1.missouri.edu).

Effect of the formation of the Isthmus of Panama on Atlantic Ocean thermohaline circulation

Gerald H. Haug* & Ralf Tiedemann

GEOMAR, Forschungszentrum für Marine Geowissenschaften, Universität Kiel, Wischhofstrasse 1-3, D-24148 Kiel, Germany

The Late Cenozoic closure of the seaway between the North and South American continents is thought to have caused extensive changes in ocean circulation and Northern Hemisphere climate[1–2]. But the timing and consequences of the emergence of the Isthmus of Panama, which closed the seaway, remain controversial[1–5]. Here we present stable-isotope and carbonate sand-fraction records from Caribbean sediments which, when compared to Atlantic and Pacific palaeoceanographic records, indicate that the closure caused a marked reorganization of ocean circulation starting 4.6 million years ago. Shallowing of the seaway intensified the Gulf Stream and introduced warm and saline water masses to high northern latitudes. These changes strengthened deep-water formation in the Labrador Sea over the next million years—as indicated by an increased deep-water ventilation and carbonate preservation in the Caribbean Sea—and favoured early Pliocene warming of the Northern Hemisphere. The evaporative cooling of surface waters during North Atlantic Deep Water formation would have introduced moisture to the Northern Hemisphere.

* Present address: Department of Earth Sciences, University of Southern California. Los Angeles, California 90089-0740, USA.

Although the pronounced intensification of Northern Hemisphere glaciation between 3.1 and 2.5 million years ago substantially lagged the full development of North Atlantic Deep Water formation, we propose that the increased atmospheric moisture content was a necessary precondition for ice-sheet growth, which was then triggered by the incremental changes in the Earth's orbital obliquity.

The gradual closing of the Isthmus of Panama lasted from 13 to 1.9 Myr ago[3–5] (all originally published ages were adjusted to the new astronomically dated timescale[6]). Most evidence for restricted water-mass exchange through the Panama strait is based on sediment records from Caribbean and Pacific Deep Sea Drilling Program (DSDP) sites 502 and 503. Significant changes in planktonic foraminiferal assemblages occur at 6.8, 4.6, 2.5 and 1.9 Myr (ref. 4). A surface-water salinity increase in the Caribbean at 4.6 Myr is indicated by $\delta^{18}O$ values of planktonic foraminifera[1] and implies a shoaling of the seaway to <100 m water depth. Shallow-water fossils from both sides of the Panama–Costa Rica region indicate[7] that the closure was almost complete at 3.6 Myr, but the final closure allowing land mammal exchange was achieved[8] at 2.7 Myr, coincident with the glacial-induced sea-level drop during the main intensification of Northern Hemisphere ice-sheet growth. However, the identification of the particular step in the closure of the Panamanian gateway that acted as a critical threshold for profound changes in deep-ocean circulation and climate remained qualitative and speculative[9]. Here we present proxy data which demonstrate that the closure has affected deep ocean circulation since 4.6 Myr ago.

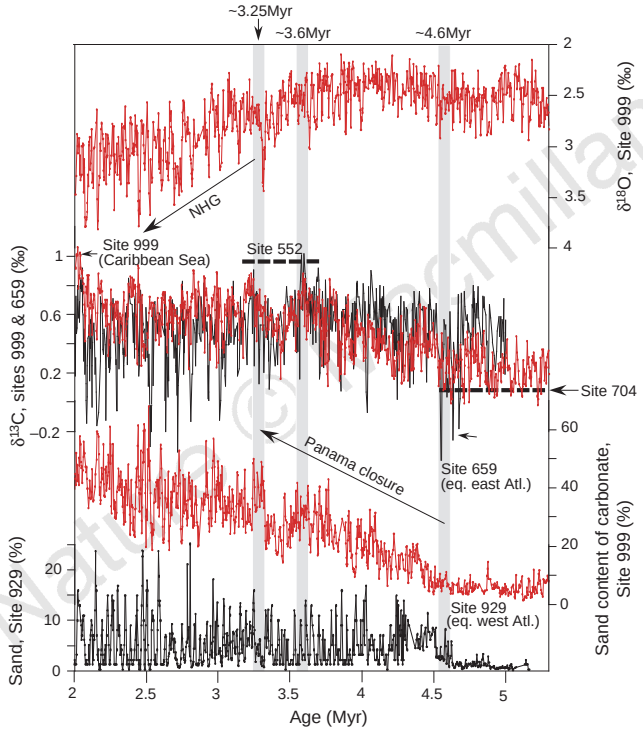

Figure 1 Palaeoceanographic records spanning the time interval 2–5.3 Myr. Top, the Site 999 isotope record (red), derived from analysing three specimens of the epibenthic foraminifera *Cibicidoides wuellerstorfi* (or if not available, *Cibicidoides kullenbergi*) of the size fraction 315–500 μm on a Finnigan MAT 252 in the stable-isotope laboratory at Geomar Kiel. $\delta^{18}O$ values are adjusted to sea water equilibrium by +0.64‰. The timescale for ODP Site 999 was achieved by adjusting the $\delta^{18}O$ fluctuations to the astronomical calibrated benthic $\delta^{18}O$ records of sites 846 (ref. 6) and 659 (ref. 15). Middle, carbon isotope records of sites 999 (red) and 659 (grey; equatorial east Atlantic; 18° 05′ N, 21° 02′ W; water depth 3,070 m). Data of both records are based on the epibenthic foraminifera *C. wuellerstorfi*. The dotted lines illustrate the average $\delta^{13}C$ values of sites 552 (ref. 17) (North Atlantic, water depth 2,301,) and 704 (ref. 16) (Southern Ocean, water depth 2,532 m). Bottom, the sand contents of sites 999 (red) and 929 (grey) (coarse fraction $>$ 63 μm); data from refs 14, 19, 33. At Site 999, the sand content is given as the percentage of total carbonate (determined with a LECO-Analyzer). The arrows mark the Pliocene cooling trend between 3.1 and 2.5 Myr (intensification of Northern Hemisphere glaciation) and the main step in Panamanian closure.

Today, a mixture of nutrient-enriched, low-$\delta^{13}C$ Antarctic Intermediate Water (AAIW) and nutrient-depleted, high-$\delta^{13}C$ Upper North Atlantic Deep Water (UNADW) and Mediterranean Overflow Water cross the Atlantic-Caribbean sills at 1,600–1,900 m (Windward Passage, Anegada-Jungfern Passage) and fill the deep Caribbean basins. During the past 2.5 Myr, the relative proportion of northern- and southern-component water masses were related to glacial–interglacial differences in the formation rate of UNADW[10]. A weaker UNADW formation during interglacials led AAIW to extend further north and result in a less ventilated, more corrosive Caribbean deep water. Hence, the Caribbean Sea is a highly sensitive recorder of ventilation changes in the upper Atlantic if the sill depth remained constant. Tectonic evidence from the Lesser Antilles arc and Aves ridge suggests no significant vertical movements since the middle Miocene (20–15 Myr ago) when a thick crust was established; vertical movements of <100 m Myr^{-1} are expected, which were likely to have been closer to a few metres per Myr (ref. 11).

We report epibenthic foraminiferal $\delta^{18}O$, $\delta^{13}C$ and percentage sand records of the carbonate fraction from ODP Site 999 (12° 44′ N, 78° 44′ W, Colombian basin, water depth 2,828 m) for the time interval 2.0–5.3 Myr. The $\delta^{13}C$ values of *Cibicidoides wuellerstorfi* are a proxy for deep-water ventilation[12], as $\delta^{13}C$ of sea water is closely linked to seawater nutrient and oxygen levels, with higher $\delta^{13}C$ values indicating lower nutrient concentrations and better ventilation[13]. The sand content ($>$63 μm) of deep-sea carbonates is a sensitive indicator of changes in carbonate dissolution. The sand content (foraminifera shells) decreases as dissolution progresses[14]. The $\delta^{18}O$ of *C. wuellerstorfi* is a proxy for changes in continental ice volume and deep water temperature. The age model of Site 999 is based on $\delta^{18}O$ stratigraphy, and was correlated to the astronomically dated $\delta^{18}O$ records from equatorial east Pacific Site 846 (ref. 6) and equatorial east Atlantic Site 659 (ref. 15).

Oceanographic conditions that result in changes in both $\delta^{13}C$ and sand contents are documented in Figs 1 and 2. Before 4.6 Myr, low epibenthic $\delta^{13}C$ values and low sand contents indicate a poorly ventilated deep Caribbean and severe carbonate dissolution. In the early Pliocene, similar low $\delta^{13}C$ values of ~0.2‰ have been

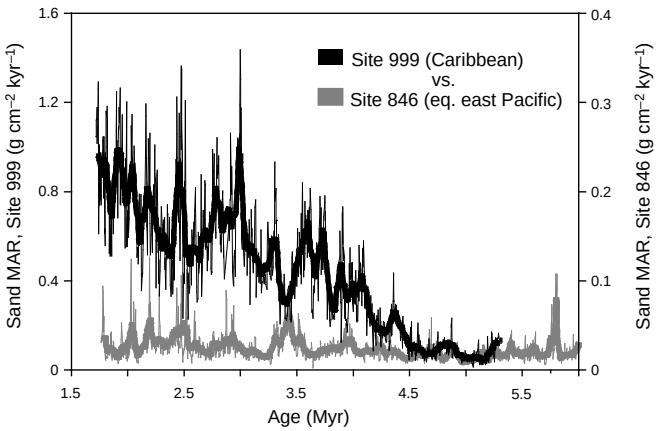

Figure 2 Comparison of carbonate sand-fraction mass accumulation rates (sand MAR) at sites 999 (left axis) and 846 (ref. 6) (right axis) plotted versus age for the interval 2–5.3 Myr. MAR are calculated by using GRAPE density values[34]. Thin lines are original data, and thick lines are data smoothed by a 20-point running mean.

documented only at subantarctic South Atlantic Site 704 (ref. 16) (2,532 m water depth), in contrast to higher North Atlantic values of ~1‰ (for example, sites 659, 552 (ref. 17)). This suggests that the Caribbean deep water was dominated by a $\delta^{13}C$-depleted Southern Ocean water mass (AAIW) before 4.6 Myr. After 4.6 Myr, deep-water ventilation as well as carbonate preservation increased into the late Pliocene due to a deepening of the lysocline. This is interpreted to reflect a progressively stronger influence of less corrosive and $\delta^{13}C$-enriched northern component water due to an increase in UNADW formation. This increase at 4.6 Myr is paralleled by an increased formation of Lower North Atlantic Deep Water (LNADW) as indicated by records of deep-water ventilation (Fig. 1) and carbonate preservation in the equatorial east (ODP sites 659 and 665 (ref. 18)) and west Atlantic (Ceara rise depth transect, sites 925–929 (ref. 19)) below 3,000 m water depth.

A first ventilation maximum in the Caribbean Sea as well as in the deep Atlantic was reached at 3.6 Myr, when Caribbean $\delta^{13}C$ values approached those from North Atlantic component water (Site 659, Fig. 1). This mechanism supplied additional heat and moisture to the Northern Hemisphere and may have contributed to the mid-Pliocene warmth. Since 3.6 Myr, both sites 999 and 659 show similar $\delta^{13}C$ maxima and reflect the increased strength of northern component water masses. During cooler periods, $\delta^{13}C$ minima at Site 659 are more pronounced than those from Caribbean Site 999 and reflect vertical fluctuations of the LNADW-AABW mixing zone (AABW, Antarctic Bottom Water). Thus, even though LNADW may have been in the 'reduced' mode during harsh climate episodes, the Caribbean was still relatively nutrient-poor compared to the deep Atlantic (Site 659) because of increased formation of UNADW. This suggests that the familiar dipole in the Pleistocene ocean circulation[10,20] has been operating at least since 3.6 Myr ago.

The comparison between the Caribbean and Pacific sand-fraction records of sites 999 and 846 demonstrates a substantial change in ocean carbonate preservation at 4.6 Myr (Fig. 2). Before 4.6 Myr, vigorous carbonate dissolution characterized both the Caribbean and the Pacific. Beginning at 4.6 Myr, the increasing thermohaline circulation amplified the inter-basin fractionation between the Atlantic and Pacific, which is reflected in a strong increase in Caribbean and Atlantic[19] carbonate preservation and a remaining strong carbonate dissolution in the Pacific. This sedimentary response to changes in ocean circulation before and after isthmus formation has been predicted by ocean model studies[21].

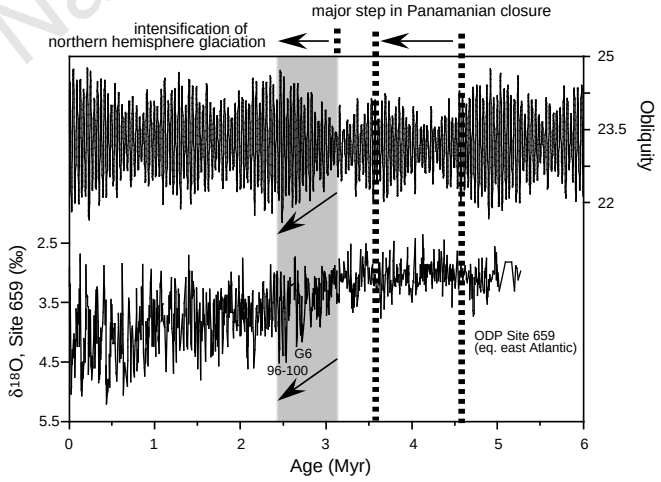

Figure 3 Calculated obliquity amplitude fluctuations[31] and the benthic oxygen isotope record of Site 659[15] versus age for the past 6 Myr. The arrows mark the Pliocene cooling trend between 3.1 and 2.5 Myr which resulted in the first large ice-sheet build-up in the Northern Hemisphere during isotopic stages G6-96 (labelled).

Our data provide a precise picture of the final phase of NADW intensification that had been developing during the mid-Miocene[22]. In response to the gradual emergence of the Central American seaway, we observe an enhanced thermohaline overturn since 4.6 Myr that reached a first maximum at 3.6 Myr. This was amplified by an increased salt transport to the North Atlantic and the initiation or intensification of UNADW formation in the Labrador Sea, as predicted by recent results[23] from global circulation model simulations. In support of this interpretation, we note that results from the Labrador Sea (ODP Leg 105) indicate increased bottom-water currents and drift sedimentation since ~4.5 Myr (ref. 24).

The closure of the Panamanian seaway has always been an attractive candidate for the ultimate cause of the Pliocene intensification of the Northern Hemisphere glaciation[9]. The pronounced ice-sheet growth in Eurasia, Greenland and North America is marked by a progressive ^{18}O-enrichment in benthic foraminifera $\delta^{18}O$ records between 3.1 and 2.5 Myr (Fig. 3) and by the massive appearance of ice-rafted debris in northern high-latitude oceans since 2.7 Myr (ref. 25). The intensification of Northern Hemisphere glaciation finalizes the Cenozoic cooling trend, which started in the early Eocene and is marked by first indications of ice sheets in Antarctica 36 Myr ago[26]. This long-term cooling is considered to be a direct response to permanent removal of atmospheric CO_2 through enhanced silicate weathering[27] and/or enhanced burial of organic carbon[28] resulting from tectonically uplifted areas such as the Himalayas and American West. This long-term cooling brought the climate system of the Earth to a state critical for ice-sheet build-up in the Northern Hemisphere. This has been the case since ~10–5 Myr ago, when the first, and minor, occurrence of ice-rafted debris in the Arctic and North Atlantic indicates the first attempts of the climate system to start a glaciation[29]. However, until 2.7 Myr ago, the climate system failed to amplify and continue a large Northern Hemisphere glaciation.

To initiate and continue the build-up of the prominent Laurentide and Scandinavian ice sheets, three factors are needed to act together. First, general cooling must have reached a critical threshold to allow precipitation to fall as snow rather than rain. Second, moisture needs to be introduced to high northern latitudes. Our results suggest that moisture was provided by an increased thermohaline circulation and Gulf Stream flow since 4.6 Myr, well before the intensification of Northern Hemisphere glaciation. Third, astronomical theory requires that the summer in northern high latitudes must be cold enough to prevent winter snow from melting[30]. High-amplitude fluctuations in the Earth's obliquity (low tilt angle) triggered cold summers in the Northern Hemisphere, and prepared the way for strengthening of the glacial–interglacial 41-kyr cycles during late Pliocene and early Pleistocene[15,30]. However, a pronounced long-term minimum in obliquity amplitude fluctuations occurred between 4.5 and 3.1 Myr (ref. 31). The $\delta^{18}O$ records of sites 659 (ref. 15), 846 (ref. 6) and 999 show that during this unfavourable orbital configuration there may have been several failed attempts of the climate system to start the glaciation, for example during 4.1–3.9 Myr and 3.5–3.3 Myr. We therefore suggest that the progressive increase in obliquity amplitudes between 3.1 and 2.5 Myr was the final trigger for amplification and continuation of the long-term expansion of Northern Hemisphere ice sheets after the necessary preconditions were met 4.6–3.6 Myr ago by formation of the Isthmus of Panama. These incremental changes in obliquity[32], coupled with changes in the background state of the ocean, suggest a threshold value for ice-sheet growth, which should be testable with climate models. □

Received 28 July 1997; accepted 14 April 1998.

1. Keigwin, L. D. Isotope paleoceanography of the Caribbean and east Pacific: role of Panama uplift in late Neogene time. *Science* **217,** 350–353 (1982).
2. Maier-Reimer, E., Mikolajewicz, U. & Crowley, T. J. Ocean general circulation model sensitivity experiment with an open American Isthmus. *Paleoceanography* **5,** 349–366 (1990).
3. Duque-Caro, H. Neogene stratigraphy, paleoceanography and paleobiology in northwest South America and the evolution of the Panama Seaway. *Palaeogeogr. Palaeoclimatol. Palaeoecol.* **77,** 203–234 (1990).

4. Keller, G., Zenker, C. E. & Stone, S. M. Late Neogene history of the Pacific-Caribbean gateway. *J. S. Am. Earth Sci.* **2,** 73–108 (1989).
5. Collins, L. S., Coates, A. G., Berggren, W. A., Aubry, M.-P. & Zhang, J. The late Miocene Panama isthmian strait. *Geology* **24,** 687–690 (1996).
6. Shackleton, N. J., Hall, M. & Pate, D. Pliocene stable isotope stratigraphy of Site 846. *Proc. ODP Sci. Res.* **138,** 337–357 (1995).
7. Coates, A. G. *et al.* Closure of the Isthmus of Panama: The near-shore marine record of Costa Rica and western Panama. *Geol. Soc. Am. Bull.* **104,** 814–828 (1992).
8. Marshall, L. G. Land mammals and the Great American Interchange. *Am. Sci.* **76,** 380–388 (1988).
9. Hay, W. W. Tectonics and climate. *Geol. Rundsch.* **85,** 409–437 (1996).
10. Oppo, D. W. *et al.* A $\delta^{13}C$ record of Upper North Atlantic Deep Water during the past 2.6 million years. *Paleoceanography* **10,** 372–394 (1995).
11. Driscoll, N. W. & Diebold, J. B. Tectonic and stratigraphic development of the eastern Caribbean: New constraints from multichannel seismic data. In *Caribbean Sedimentary Basins* (ed. Mann, P.) (Elsevier Spec. Publ., in the press).
12. McCorkle, D. C. & Keigwin, L. D. Depth profiles of $\delta^{13}C$ in bottom water and core top *C. wuellerstorfi* on the Ontong Java Plateau and Emperor Seamounts. *Paleoceanography* **9,** 197–208 (1994).
13. Kroopnick, P. M. The distribution of ^{13}C of ΣCO_2 in the world ocean. *Deep-Sea Res.* **32,** 57–84 (1985).
14. Bickert, T., Cordes, R. & Wefer, G. Late Pliocene to mid-Pleistocene (2.6–1.0 Ma) carbonate dissolution in the western equatorial Atlantic: Results of ODP Leg 154, Ceara Rise. *Proc. ODP Sci. Res.* **154** (1994).
15. Tiedemann, R., Sarnthein, M. & Shackleton, N. J. Astronomic timescale for the Pliocene Atlantic $\delta^{18}O$ and dust flux records of ODP Site 659. *Paleoceanography* **9,** 619–638 (1994).
16. Hodell, D. A., Müller, D. W., Ciesielski, P. F. & Mead, G. A. Synthesis of oxygen and carbon isotopic results from Site 704: Implications for major climatic-geochemical transitions during the late Neogene. *Proc. ODP Sci. Res.* **114,** 475–480 (1991).
17. Shackleton, N. J. & Hall, M. A. Oxygen and carbon isotope stratigraphy of DSDP Hole 552A: Pliocene-Pleistocene glacial history. *Init. Rep. DSDP* **81,** 599–610 (1984).
18. Ruddiman, W. F. *et al. Proc. ODP Init. Rep.* **108** (1988).
19. Tiedemann, R. & Franz, S. O. Deep-water circulation, chemistry, and terrigenous sediment supply in the equatorial Atlantic during the Pliocene, 3.3–2.6 Ma and 5–4.5 Ma. *Proc. ODP Sci. Res.* **154,** 299–318 (1997).
20. Boyle, E. A. & Keigwin, L. D. North Atlantic thermohaline circulation during the past 20,000 years linked to high-latitude surface temperature. *Nature* **330,** 35–40 (1987).
21. Heinze, C. & Crowley, T. J. Sedimentary response to ocean gateway circulation changes. *Paleoceanography* **12,** 742–754 (1997).
22. Wright, J. D. & Miller, K. G. Control of North Atlantic Deep Water circulation by the Greenland-Scotland Ridge. *Paleoceanography* **11,** 157–171 (1996).
23. Mikolajewicz, U. & Crowley, T. J. Response of a coupled ocean/energy balance model to restricted flow through the central American Isthmus. *Paleoceanography* **12,** 429–441 (1997).
24. Arthur, M. A. *et al.* Seismic stratigraphy and history of deep circulation and sediment drift development in Baffin Bay and the Labrador Sea. *Proc. ODP Sci. Res.* **105,** 957–989 (1989).
25. Shackleton, N. J. *et al.* Oxygen isotope calibration of the onset of ice-rafting and history of glaciation in the North Atlantic region. *Nature* **307,** 620–623 (1984).
26. Miller, K. G., Fairbanks, R. G. & Mountain, G. S. Tertiary oxygen isotope synthesis, sea level history, and continental margin erosion. *Paleoceanography* **2,** 1–19 (1987).
27. Raymo, M. E. & Ruddiman, W. F. Tectonic forcing of late Cenozoic climate. *Nature* **359,** 117–122 (1992).
28. France-Lanord, C. & Derry, L. A. Organic carbon burial forcing of the carbon cycle from Himalayan erosion. *Nature* **390,** 65–67 (1997).
29. Myhre, A. M. *et al. Proc. ODP Init. Rep.* **151,** 1–926 (1996).
30. Imbrie, J. *et al.* On the structure and origin of major glaciation cycles, 1. linear responses to Milankovitch forcing. *Paleoceanography* **7,** 701–738 (1992).
31. Laskar, J., Joutel, F. & Boudin, F. Orbital, precessional, and insolation quantities for the Earth from −20 Myr to +10 Myr. *Astron. Astrophys.* **270,** 522–533 (1993).
32. Li, X. S. *et al.* Simulating late Pliocene Northern Hemisphere climate with the LLN 2-D model. *Geophys. Res. Lett.* (in the press).
33. Billups, K., Ravelo, A. C. & Zachos, J. C. Early Pliocene deep-water circulation: Stable isotope evidence for enhanced northern component deep water. *Proc. ODP Sci. Res.* **154,** 319–330 (1997).
34. Sigurdsson, H. *et al. Proc. ODP Init. Rep.* **165,** 1–674 (1997).

Acknowledgements. We thank R. Zahn, S. Franz, L. Keigwin, D. Oppo, N. Driscoll, R. Norris, J. McManus and T. Bickert for discussions and criticism, and S. Hustedt and A. Richter for technical assistance. This work was supported by the Deutsche Forschungsgemeinschaft (DFG).

Correspondence and requests for materials should be addressed to G.H.H. (e-mail: ghaug@earth.usc.edu).

Palaeozoic and Proterozoic zircons from the Mid-Atlantic Ridge

Joachim Pilot, Carl-Dietrich Werner, Frank Haubrich & Nils Baumann

Institute of Mineralogy, Freiberg University of Mining and Technology, D-09596 Freiberg, Germany

According to the theory of plate tectonics, rocks found in the vicinity of mid-ocean ridges—where oceanic plates are created—should be relatively young (at most several Myr old). Here we report the discovery of zircons with ages of about 330 and 1,600 Myr that were drilled from exposed gabbros beneath the Mid-Atlantic Ridge near the Kane fracture zone[1–4]. Age determinations were made using the $^{207}Pb/^{206}Pb$ evaporation method[5] and confirmed with conventional U–Pb dating and ion microprobe (SHRIMP) analysis. We suggest two plausible explanations for the origin of these unusually old zircons. During the opening of the Atlantic, sheared crustal material or delaminated continental lithosphere sank into small roll-like circulation cells[6,7] that developed in the shallow mantle at each side of the ridge axis and the material was then transported through these cells to the ridge axis. Alternatively, material from the continental crust has been trapped within the Kane fracture zone since the opening of the Atlantic Ocean basin through a series of transform migrations and ridge jumps[8,9], with portions of this material subsequently migrating down the ridge axis.

Leg 153 of the Ocean Drilling Program drilled five sites on the western valley wall of the Mid-Atlantic Ridge (MAR) between 23° 20′ N and 23° 30′ N, 5–35 km south of the Kane transform (Fig. 1). This area is located in the central Atlantic Ocean, ~2,000 km from the continental margins and far from any islands. Leg 153 recovered harzburgites of the upper mantle which are depleted by partial melting followed by the formation of gabbroic melts[1–4]. The peridotite–harzburgite–gabbro complex is interpreted to be uplifted and exhumed by normal faults[1–4,10,11]. The gabbros comprise normal gabbro, olivine gabbro, gabbronorite, olivine gabbronorite, olivine norite, and troctolite.

From the recovered cores, we selected 30 gabbro samples from material drilled 7.7–68.9 m below the sea floor. These samples were the least altered ones and did not contain visible schlieren and veins.

While performing oxygen-isotope investigations of these gabbro samples, we discovered numerous zircons. Some of these samples contain 1–4 zircons in 5 cm^3; however, close to 40 zircons were found in sample 137. The number of zircons identified does not correspond to the Zr content of the host rock (mean ~20 p.p.m.). The morphology of zircons in samples from the same borehole is similar, but differs in samples from different boreholes. Most of the zircons are 20–60 μm in size, yellow-white and transparent with some reddish tear-type inclusions, and sometimes show a lineation parallel to crystal faces (Fig. 2). Frequent types in the Pupin diagram[12] are P1, P2, G1 and G2, with short prismatic shapes being most abundant. Sample 122 from borehole 922A contained zircons that were of irregular, or had no discernible, shape.

Zircons in gabbro complexes which occur mainly in veinlets and schlieren have been reported several times[10,11,13–15]. In thin sections such zircons are seen at the borders between mineral grains; in one case, a zircon was included in an ilmenite grain[13]. However, our sampling avoided visible veins, schlieren and any signs of alteration as far as possible; the zircons used for our age determinations are clearly different from those which may be formed in the highly differentiated rest-magma of the gabbroic melts.

If the zircons were formed during the generation of the gabbroic magma, then their age would be expected to be ~1 Myr (ref. 1); because of their U contents it would be difficult to determine a U–Pb age. To reveal the history of these zircons, we first made $^{207}Pb/^{206}Pb$ age determinations of carefully selected single zircons from three samples (samples 134 and 137, borehole 923A; sample 122, borehole 922A), using the well established mass-spectrometric evaporation method[5].

All zircons contain both radiogenic lead and small, but significant,

Table 1 Isotope ratios of zircons from sample 122

Sample	$^{204}Pb/^{206}Pb_m$	$^{207}Pb/^{206}Pb_m$	$^{208}Pb/^{206}Pb_m$	$^{206}Pb/^{238}U$	$^{207}Pb/^{235}U$
122/L14-1	0.002401(18)	0.13038(17)	0.14305(23)	0.2022(16)	2.714(37)
122/L14-2	0.002606(16)	0.12967(12)	0.13313(27)	0.1821(25)	2.353(45)
122/L14-3	0.002516(32)	0.13605(12)	0.20123(24)	0.2552(21)	3.584(58)

Shown are lead isotope ratios and corrected $^{206}Pb/^{238}U$ and $^{207}Pb/^{235}U$ ratios from sample 122 zircons (second separation). (Subscript m indicates measured ratio but mass spectrometric discrimination is corrected).